Research Article
Molecular and Cell Biology

JOURNAL
OF HEPATOLOGY

$G\alpha_{12}$ overexpression induced by miR-16 dysregulation contributes to liver fibrosis by promoting autophagy in hepatic stellate cells

Graphical abstract

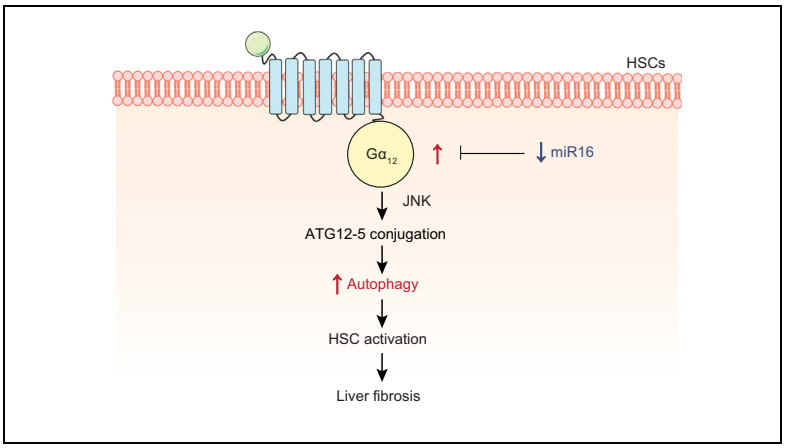

Highlights

- $G\alpha_{12}$ expression was enhanced during HSC activation due to miR-16 dysregulation.
- $G\alpha_{12}$ signaling facilitates autophagy via JNK-dependent ATG12-5 formation.
- $G\alpha_{12}$ associated molecules in HSCs may serve as targets for fibrosis treatment.

Authors

Kyu Min Kim, Chang Yeob Han, Ji Young Kim, ..., Se Jin Hwang, Sung Hwan Ki, Sang Geon Kim

Correspondence

sgk@snu.ac.kr (S.G. Kim)

Lay summary

Guanine nucleotide-binding α-subunit 12 ($G\alpha_{12}$) is upregulated in activated hepatic stellate cells (HSCs) as a consequence of the dysregulation of a specific microRNA that is abundant in HSCs, facilitating the progression of liver fibrosis. This event is mediated by c-Jun N-terminal kinase-dependent ATG12-5 formation and the promotion of autophagy. We suggest that $G\alpha_{12}$ and its associated regulators could serve as new targets in HSCs for the treatment of liver fibrosis.

http://dx.doi.org/10.1016/j.jhep.2017.10.011
 J. Hepatol. 2018, 68, 493–504

Research Article
Molecular and Cell Biology

JOURNAL OF HEPATOLOGY

$G\alpha_{12}$ overexpression induced by miR-16 dysregulation contributes to liver fibrosis by promoting autophagy in hepatic stellate cells

Kyu Min Kim[1], Chang Yeob Han[1], Ji Young Kim[2], Sam Seok Cho[2], Yun Seok Kim[1], Ja Hyun Koo[1], Jung Min Lee[1], Sung Chul Lim[3], Keon Wook Kang[1], Jae-Sung Kim[4], Se Jin Hwang[5], Sung Hwan Ki[2], Sang Geon Kim[1,*]

[1]*College of Pharmacy and Research Institute of Pharmaceutical Sciences, Seoul National University, Seoul 08826, Republic of Korea;* [2]*College of Pharmacy, Chosun University, Gwangju 61452, Republic of Korea;* [3]*College of Medicine, Chosun University, Gwangju 61452, Republic of Korea;* [4]*Departments of Surgery University of Florida, Gainesville, FL 32611, USA;* [5]*College of Medicine, Hanyang University, Seoul 04763, Republic of Korea*

Background & Aims: Hepatic stellate cells (HSCs) have a role in liver fibrosis. Guanine nucleotide-binding α-subunit 12 ($G\alpha_{12}$) converges signals from G-protein-coupled receptors whose ligand levels are elevated in the environment during liver fibrosis; however, information is lacking on the effect of $G\alpha_{12}$ on HSC *trans*-differentiation. This study investigated the expression of $G\alpha_{12}$ in HSCs and the molecular basis of the effects of its expression on liver fibrosis.

Methods: $G\alpha_{12}$ expression was assessed by immunostaining, and immunoblot analyses of mouse fibrotic liver tissues and primary HSCs. The role of $G\alpha_{12}$ in liver fibrosis was estimated using a toxicant injury mouse model with *$G\alpha_{12}$* gene knockout and/or HSC-specific $G\alpha_{12}$ delivery using lentiviral vectors, in addition to primary HSCs and LX-2 cells using microRNA (miR) inhibitors, overexpression vectors, or adenoviruses. miR-16, $G\alpha_{12}$, and LC3 were also examined in samples from patients with fibrosis.

Results: $G\alpha_{12}$ was overexpressed in activated HSCs and fibrotic liver, and was colocalised with desmin. In a carbon tetrachloride-induced fibrosis mouse model, $G\alpha_{12}$ ablation prevented increases in fibrosis and liver injury. This effect was attenuated by HSC-specific lentiviral delivery of $G\alpha_{12}$. Moreover, $G\alpha_{12}$ activation promoted autophagy accompanying c-Jun N-terminal kinase-dependent ATG12-5 conjugation. In addition, miR-16 was found to be a direct inhibitor of the *de novo* synthesis of $G\alpha_{12}$. Modulations of miR-16 altered autophagy in HSCs. In a fibrosis animal model or patients with severe fibrosis, miR-16 levels were lower than in their corresponding controls. Consistently, cirrhotic patient liver tissues showed $G\alpha_{12}$ and LC3 upregulation in desmin-positive areas.

Conclusions: miR-16 dysregulation in HSCs results in $G\alpha_{12}$ overexpression, which activates HSCs by facilitating autophagy through ATG12-5 formation. This suggests that $G\alpha_{12}$ and its regulatory molecules could serve as targets for the amelioration of liver fibrosis.

Lay summary: Guanine nucleotide-binding α-subunit 12 ($G\alpha_{12}$) is upregulated in activated hepatic stellate cells (HSCs) as a consequence of the dysregulation of a specific microRNA that is abundant in HSCs, facilitating the progression of liver fibrosis. This event is mediated by c-Jun N-terminal kinase-dependent ATG12-5 formation and the promotion of autophagy. We suggest that $G\alpha_{12}$ and its associated regulators could serve as new targets in HSCs for the treatment of liver fibrosis.

Introduction

Liver fibrosis is a scarring response promoting the deposition of extracellular matrix (ECM) components against hepatocyte injury.[1] ECM deposition disturbs normal liver function and architecture and can progress to liver cirrhosis when left untreated. When exposed to various external stimuli during chronic injury, hepatic stellate cells (HSCs) are primarily responsible for the disproportionate fibre accumulation that leads to liver fibrosis. Additionally, HSCs cause ECM deposition through *trans*-differentiation from a quiescent phenotype to a myofibroblastic phenotype.[2] However, there is currently no clinically effective way to inhibit HSC activation and fibrosis progression;[3] therefore, identification of the regulatory molecules and mechanisms involved in this process could assist in the implementation of new diagnostic and therapeutic targets related to liver fibrosis.

Given their roles in complex biological processes, increased attention has been paid to G-protein-coupled receptors (GPCRs), which recognise extracellular ligands, and their related downstream molecules and pathways.[4] GPCR activation and subsequent downstream activity is promoted by guanine nucleotide-binding α-subunits (Gα) proteins. Among these, $G\alpha_{12}$ has attracted particular interest owing to its potent transforming capacity. Specifically, $G\alpha_{12}$ transduces signals to control cell proliferation, migration, and inflammation.[5,6] Additionally, ligands that promote specific GPCR coupling to $G\alpha_{12}$ [*i.e.* sphingosine-1-phosphate (S1P), lysophosphatidic acid, angiotensin 2 (Ang II), thrombin, and endothelin-1] are implicated in liver fibrosis.[7,8] Given that $G\alpha_{12}$ converges signals from multiple GPCRs and coordinates GPCR-specific signalling cascades

Keywords: Liver fibrosis; Activated stellate cell; G protein; Non-coding RNA; Lysosomal degradation.
Received 31 October 2016; received in revised form 10 October 2017; accepted 11 October 2017; available online 2 January 2018
* Corresponding author. Address: College of Pharmacy, Seoul National University, Gwanakro-1, Seoul 08826, Republic of Korea.
E-mail address: sgk@snu.ac.kr (S.G. Kim).

to common downstream molecules,[9] $G\alpha_{12}$ levels could have a profound effect on the blunting or amplification of biochemical and physiological activities.

Autophagy is an essential catabolic process involved in lysosomal degradation and recycling of intracellular organelles and proteins to maintain cellular homeostasis. In HSCs, autophagy increases the fibrogenic response through the breakdown of lipid droplets.[10] Autophagy is orchestrated by events and proteins, including microtubule-associated protein 1 light chain 3 (LC3), and autophagy-related gene (ATG)12-5 and ATG16, with LC3-II being necessary for membrane extension and closure to form vesicles.[11] In HSCs, autophagy is activated by many ligands of GPCRs that interact with $G\alpha_{12}$;[12,13] therefore, we hypothesised that $G\alpha_{12}$ could affect autophagy.

Given the lack of understanding of the role of $G\alpha_{12}$ in HSC *trans*-differentiation and the potential link between

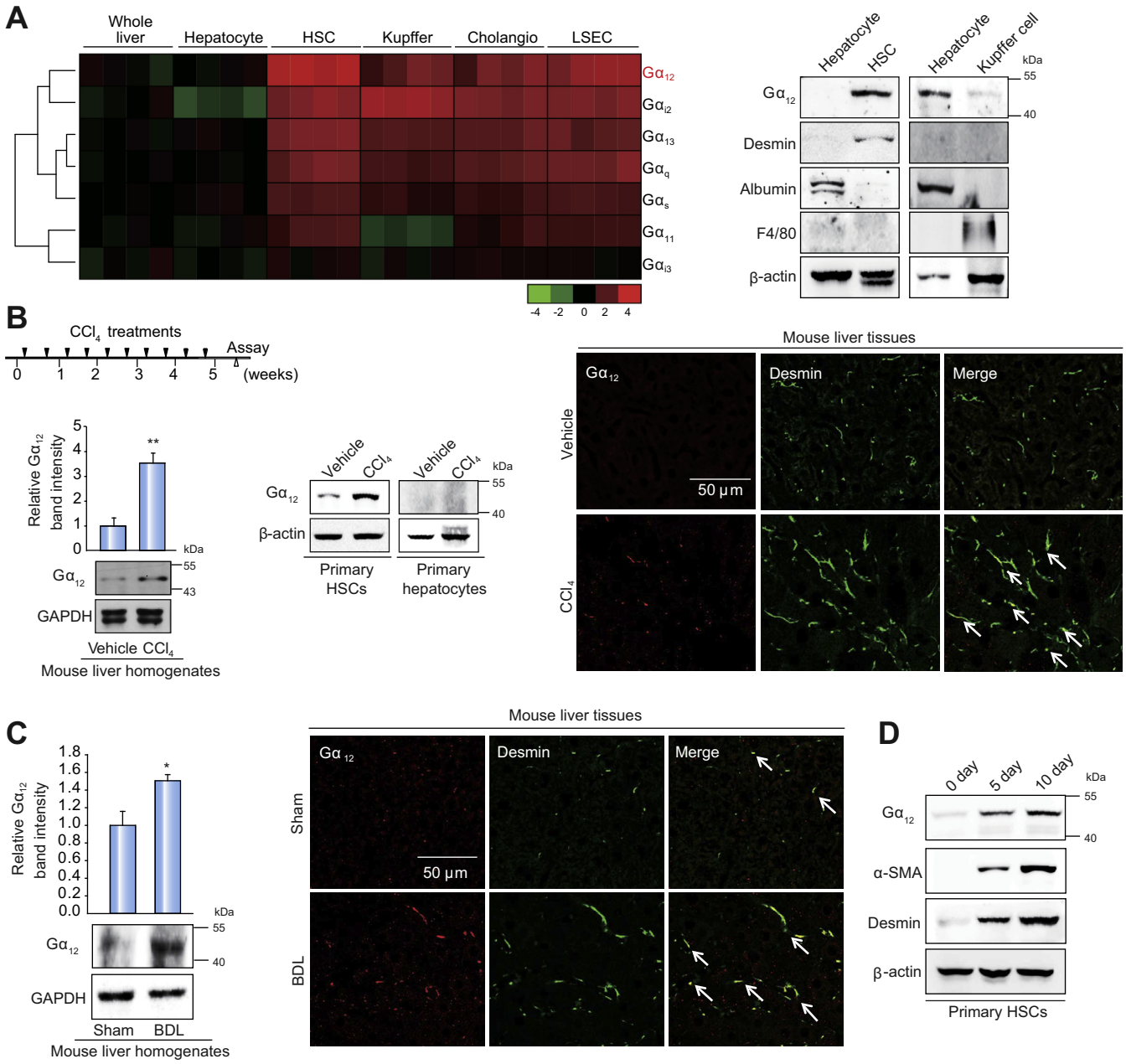

Fig. 1. $G\alpha_{12}$ is overexpressed in activated HSCs and in fibrotic liver tissue. (A) Left: heat map of Gα subunits in the whole liver or individual hepatic cells. Data were extracted from a cell-type-resolved proteomics atlas of the mouse liver. Protein levels were normalised by their expression in whole-liver homogenates. Right: immunoblottings on the lysates of freshly isolated mouse hepatocytes, HSCs, and Kupffer cells. The difference in band intensity in hepatocytes was the result of the exposure time. (B) Left: immunoblotting for $G\alpha_{12}$. Mice were injected with vehicle (corn oil) or CCl_4 for five weeks (n = 4–6 each). Middle: immunoblotting on quiescent HSCs and hepatocytes freshly isolated from mice 24 h after a single dose of CCl_4. Right: Immunostaining (scale bar: 50 µm). White arrows indicate $G\alpha_{12}$ and desmin colocalisation. (C) Left: immunoblotting for $G\alpha_{12}$ (n = 3 each). Right: Immunostaining. (D) Immunoblottings on quiescent (freshly isolated), or culture-activated (5 or 10 days) primary HSCs. (B,C) Values represent the mean ± SEM. The statistical significance of the differences between each treatment and vehicle group (*p <0.05 and **p <0.01, significant *vs.* respective controls) was determined by a two-tailed t test. α-SMA, alpha-smooth muscle actin; CCl_4, carbon tetrachloride; $G\alpha_{12}$, guanine nucleotide-binding α-subunit 12; GAPDH, glyceraldehyde 3-phosphate dehydrogenase; HSC, hepatic stellate cell. (This figure appears in colour on the web.)

$G\alpha_{12}$ and autophagy, this study investigated whether $G\alpha_{12}$ is upregulated in HSCs and, if so, what its impact is on liver fibrosis and how it is regulated in conjunction with autophagy. Our results showed that $G\alpha_{12}$ is overexpressed in activated HSCs because of the dysregulation of a specific microRNA (miR) that is abundant in HSCs, facilitating liver fibrosis. In addition, HSC-specific delivery of $G\alpha_{12}$ to whole-body *$G\alpha_{12}$* knockout (KO) mice or wild-type (WT) mice using two different sets of constructs confirmed the role of $G\alpha_{12}$ overexpression in HSCs in the progression of fibrosis. Moreover, our findings indicated that this event was mediated by c-Jun N-terminal kinase (JNK)-dependent ATG12-5 formation and the induction of autophagy.

Materials and methods

Materials

Information on the materials used in this study is provided in the Supplementary Material online.

Animal treatment

The protocol for the animal experiments was approved by the Institutional Animal Use and Care Committee at Seoul National University, and followed ARRIVE guidelines. Detailed information is provided in the Supplementary material online.

Targeted gene delivery

Lentiviral SMA-$G\alpha_{12}$ and SMA-$G\alpha_{12}$-enhanced green fluorescence protein (EGFP) were cloned, and the viruses produced were administered to C57BL/6 mice via tail vein for HSC-specific gene delivery. Specific details are provided in the Supplementary material online.

For further details regarding the materials used, please refer to the CTAT table and Supplementary information.

Results

$G\alpha_{12}$ is overexpressed in HSCs and fibrotic liver

We analysed Gα-isoform levels in different types of liver-resident cell using the proteome data from whole liver and individual hepatic cell types.[14] Of the proteins detected in whole-liver lysates, $G\alpha_{12}$ showed the highest signal intensities specifically in HSCs (Fig. 1A, left). We compared $G\alpha_{12}$ levels in primary cell types isolated from the liver of healthy mice, and found that $G\alpha_{12}$ was more abundant in HSCs than in hepatocytes. In addition, hepatocytes expressed $G\alpha_{12}$ to a greater extent than did Kupffer cells (Fig. 1A, right). Desmin$^+$ and F4/80$^-$ staining validated the purity of HSCs (Fig. S1). To understand the link between $G\alpha_{12}$ and liver fibrosis, we examined $G\alpha_{12}$ levels in animal models. $G\alpha_{12}$ was overexpressed in liver homogenates prepared from mice treated with carbon tetrachloride (CCl_4) (Fig. 1B, left). Additionally, $G\alpha_{12}$ was upregulated in HSCs isolated from mice treated with CCl_4. This effect was not seen in primary hepatocytes (Fig. 1B, middle). Moreover, $G\alpha_{12}$ was enhanced and colocalised with desmin in fibrotic liver samples, confirming the overexpression of $G\alpha_{12}$ in activated HSCs (Fig. 1B, right). The same changes occurred in animals with bile duct ligation (Fig. 1C). $G\alpha_{12}$ levels gradually increased in primary HSCs during culture activation, with induction of alpha-smooth muscle actin (α-SMA) and desmin (Fig. 1D). Our data showed that $G\alpha_{12}$ was overexpressed in both fibrotic livers and activated HSCs. Analysis of the human Gene Expression Omnibus database (GSE25097) revealed that the transcript levels of GPCRs capable of interacting with $G\alpha_{12}$ members were higher in patients with liver cirrhosis compared with those in healthy individuals (Fig. S2A).

We then used S1P as a representative GPCR ligand to activate $G\alpha_{12}$ to examine the role of $G\alpha_{12}$ in HSC activation; *$G\alpha_{12}$*

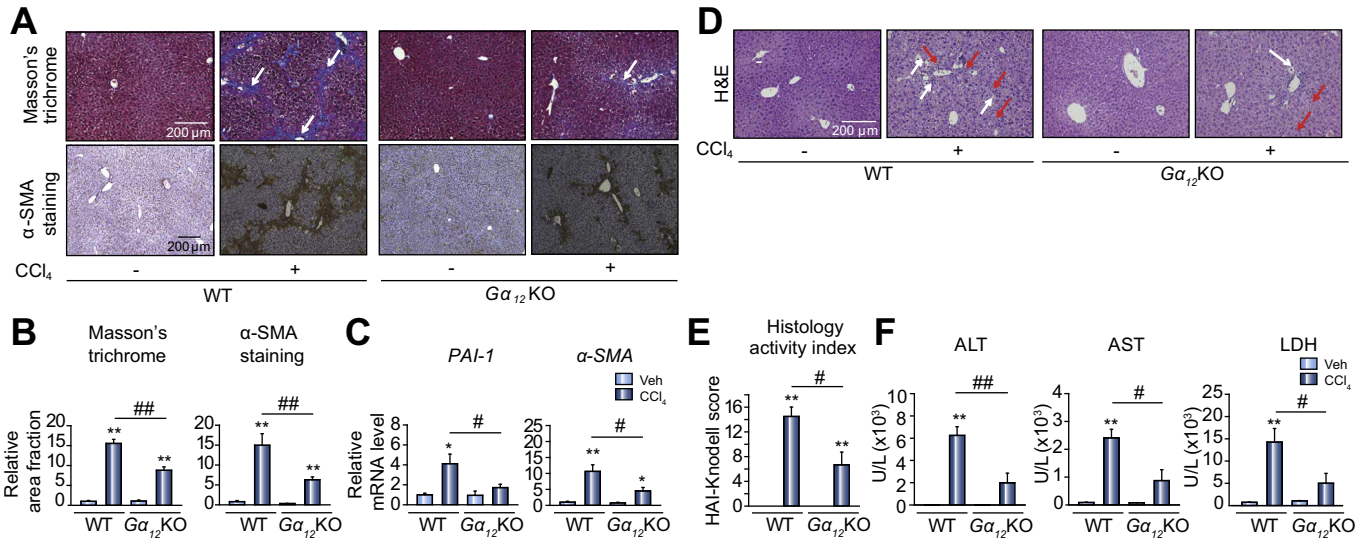

Fig. 2. Liver fibrosis is inhibited by *$G\alpha_{12}$* KO. (A) Upper: Masson's trichrome staining. Mice were treated as in the legend of Fig. 1B (n = 4–6 each). White arrows indicate periportal fibrosis (scale bar: 200 μm). Lower: immunostaining (scale bar: 200 μm) (n = 4–6 each). (B) Relative staining area fractions using image analysis software. (C) qRT-PCR assays (n = 4–6 each). (D) H&E staining. White arrows indicate vacuolar degeneration of hepatocytes, whereas red arrows show inflammatory cell infiltration in the periportal area (scale bar: 200 μm) (n = 4–6 each). (E) HAI-Knodell scores (n = 4–6 each). (F) Serum enzyme activities (n = 4–6 each). (B, C, E, F) Values represent the mean ± SEM. The statistical significance of the differences was determined by a two-tailed *t* test (**p* <0.05 and ***p* <0.01, significant *vs.* vehicle-treated WT mice; #*p* <0.05 and ##*p* <0.01, significant *vs.* CCl_4-treated WT mice). α-SMA, alpha-smooth muscle actin; CCl_4, carbon tetrachloride; $G\alpha_{12}$, guanine nucleotide-binding α-subunit 12; HSC, hepatic stellate cell; LDH, lactate dehydrogenase; qRT-PCR, quantitative reverse transcription PCR; WT, wild-type. (This figure appears in colour on the web.)

knockdown prevented S1P from inducing α-SMA (Fig. S2B), supporting the idea that $G\alpha_{12}$ mediates the GPCR activation of HSCs. This effect of $G\alpha_{12}$ knockdown was not seen in vehicle-treated cells because of the lack of GPCR activation (*i.e.* unactivated state). These results provide evidence that $G\alpha_{12}$ is overexpressed in activated HSCs, resulting in liver fibrosis.

$G\alpha_{12}$ ablation improves liver fibrosis

To assess the effect of $G\alpha_{12}$ overexpression on liver fibrosis and the accompanying hepatocyte injuries, we introduced a toxicant-induced fibrosis model using WT and $G\alpha_{12}$ KO mice. In Masson's trichrome- and α-SMA-staining assays, ECM accumulation was attenuated in the livers of $G\alpha_{12}$ KO mice

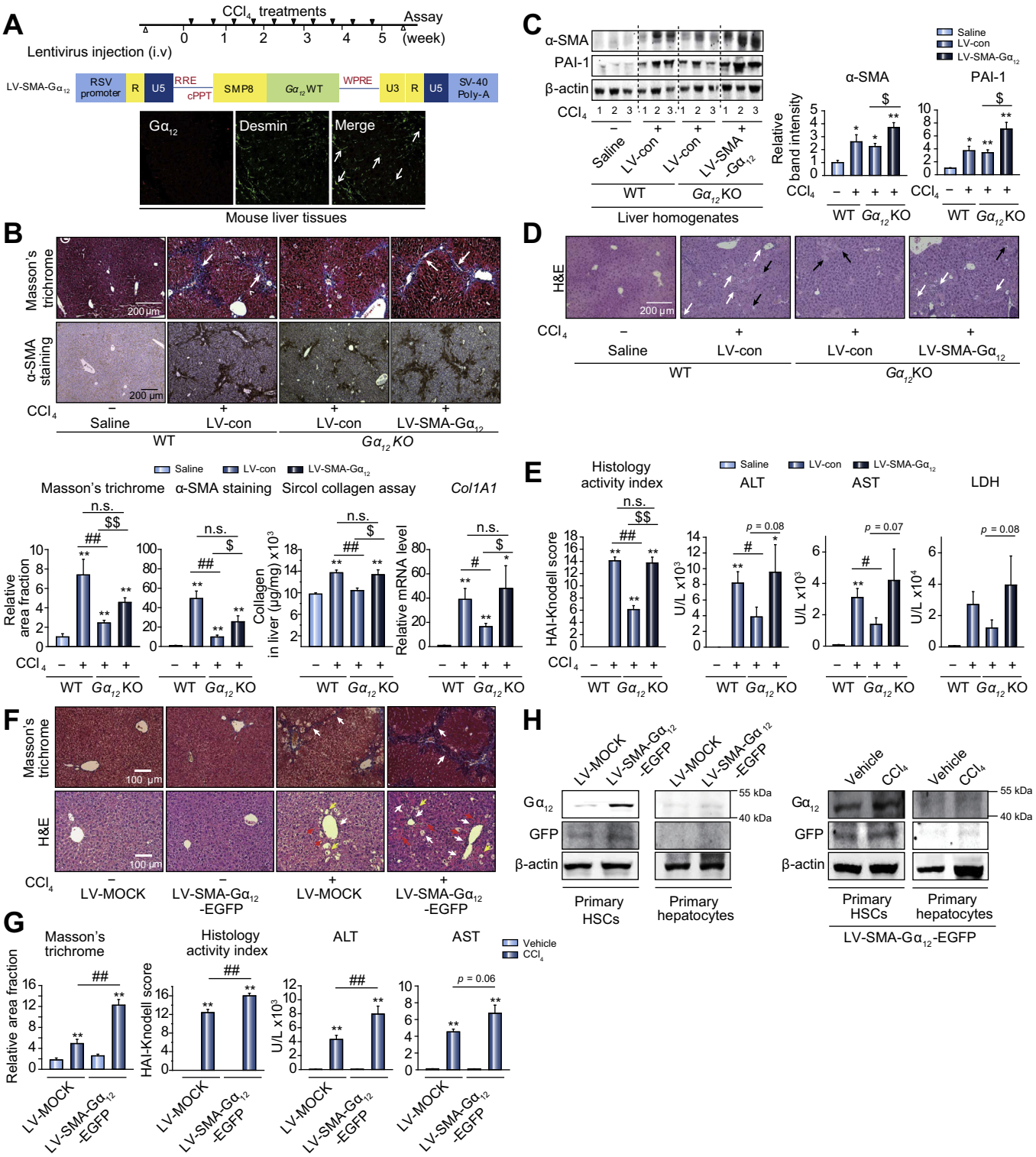

compared with corresponding controls (Fig. 2A,B). This effect was confirmed by qRT-PCR assays for plasminogen activator inhibitor-1 (PAI-1) and α-SMA (Fig. 2C). Additionally, *Gα12* KO ameliorated histopathological changes, including hepatocyte vacuolar degeneration and inflammatory cell infiltration (Fig. 2D). Consistently, HAI-Knodell scores and ALT, AST, and lactate dehydrogenase (LDH) activities were all significantly decreased in *Gα12* KO mice (Fig. 2E,F). These results provided evidence that $G\alpha_{12}$ ablation diminishes toxicant-induced liver fibrosis and hepatocyte injury.

Lentiviral delivery of $G\alpha_{12}$ to HSCs exacerbates liver fibrosis

To ascertain the effect of $G\alpha_{12}$ overexpression in HSCs on liver fibrosis, we created a lentiviral SMA-$G\alpha_{12}$ (LV-SMA-$G\alpha_{12}$) delivery system (*i.e.* a construct comprising the gene encoding *Gα12* downstream from the α-SMA promoter) to accomplish HSC-specific $G\alpha_{12}$ overexpression (Fig. 3A). This system had been used for HSC-specific gene delivery in our previous studies, and its specificity had been previously validated.[15] As expected, HSC-specific gene delivery resulted in $G\alpha_{12}$ overexpression and its colocalisation with desmin (Fig. 3A). Notably, $G\alpha_{12}$ overexpression in HSCs considerably attenuated the beneficial effect of *Gα12* KO on fibrosis, as shown by Masson's trichrome and α-SMA staining, Sircol Collagen assays, and qRT-PCR for collagen 1A1 in the liver (Fig. 3B), with immunoblot results for α-SMA and PAI-1 in liver homogenates verifying this outcome (Fig. 3C).

WT mice showed fibre accumulation, ballooning degeneration, and hepatocyte necrosis in the periportal area, piecemeal necrosis of hepatocytes, and infiltration of inflammatory cells in the liver (Fig. 3D). HSC-specific $G\alpha_{12}$ overexpression in *Gα12* KO mice diminished histopathological improvements, as verified by changes in the HAI-Knodell score. Similar tendencies were obtained for serum ALT, AST, and LDH activities (Fig. 3E). In addition, HSC-specific $G\alpha_{12}$ overexpression in *Gα12* KO mice diminished the protective effect of *Gα12* KO on hepatic inflammation, as indicated by changes in a macrophage marker (*i.e.* F4/80) and portal inflammation scores (Fig. S3). To confirm the effect of HSC-specific gene delivery, another set of lentiviral constructs (LV-SMA-$G\alpha_{12}$-EGFP and LV-MOCK) were created and utilised in WT mice (Fig. S4A). $G\alpha_{12}$ overexpression in HSCs augmented collagen accumulation in mice treated with CCl_4 for two weeks (Fig. 3F, upper). Histopathology changed consistently (Fig. 3F, lower), as corroborated by HAI-Knodell scores and serum aminotransferase activities (Fig. 3G). Immunoblotting for α-SMA in liver homogenates also confirmed the activating effect of $G\alpha_{12}$ on HSCs (Fig. S4B). Cell-specific gene delivery was validated using HSCs and hepatocytes isolated from healthy mice injected with the constructs (Fig. 3H, left). CCl_4 treatments *in vivo* did not affect the efficiency of lentivirus-mediated gene expression, as shown by a minimal change in GFP level in primary HSCs, although a slight increase in $G\alpha_{12}$ intensity could reflect an increase in the amount of endogenous protein upon CCl_4 treatment (Fig. 3H, right). These results confirmed that HSC-specific $G\alpha_{12}$ overexpression is sufficient to promote liver fibrosis.

Induction of autophagy by $G\alpha_{12}$

Autophagy is associated with the establishment of activated HSC phenotypes responsible for liver fibrosis.[10,16] We hypothesised that $G\alpha_{12}$ overexpression might facilitate autophagy. As expected, culture activation of primary HSCs enhanced LC3B-II (Fig. 4A, left). The level of p62 increased along with LC3B-II after chloroquine treatment, which could reflect the accumulation of these proteins under our experimental conditions. Nevertheless, the increase of p62 remains to be studied further (*e.g.* the regulation of p62 by the $G\alpha_{12}$ signalling network).[17] In animals, $G\alpha_{12}$ ablation completely prevented CCl_4 *in vivo* treatment from increasing LC3B-II in isolated primary HSCs (Fig. 4A, middle). Consistently, $G\alpha_{12}$ overexpression *in vivo* promoted LC3B-II in the primary HSCs (Fig. S5A). Moreover, a decrease in autophagic flux by *Gα12* KO was visualised by fluorescence analysis using adenoviral mCherry-GFP-LC3, a tool used to monitor LC3 flux (GFP fluorescence is quenched in the acidic lysosomal environment, whereas the red fluorescence of mCherry remains evident under such conditions). We observed that the number of mCherry red puncta was diminished in *Gα12* KO primary HSCs compared with controls (Fig. 4B), where yellow and red fluorescence represented autophagosomes and autolysosomes, respectively.[18] Consistently, ectopic overexpression of an active mutant of $G\alpha_{12}$ ($G\alpha_{12}$QL) increased LC3B-II in LX-2 cells (Fig. 4C, left). Additionally, exposure of cells to 3-methyladenine, a pharmacological inhibitor of autophagy, prohibited this effect (Fig. 4C, right lower). Therefore, these findings implied $G\alpha_{12}$ mediated autophagy promotion. Immunoblots for α-SMA or PAI-1 showed appropriate changes in HSC activation in accordance with $G\alpha_{12}$ (Fig. 4A, right and 4C, right upper), confirming the link between autophagy and HSC activation.

Fig. 3. HSC-specific lentiviral delivery of $G\alpha_{12}$ exacerbates liver fibrosis. (A) Schematic showing a construct encoding WT-*Gα12* (LV-SMA-*Gα12*) downstream from the mouse *α-sma* promoter (SMP8). Mice were injected with each construct (or saline) through the tail vein. After 1 week, they were subjected to CCl_4 treatment for five weeks (n = 3–9 each). Immunostaining for $G\alpha_{12}$ and desmin confirmed colocalisation (magnification: 40×). (B) Upper: Masson's trichrome staining. Symbols represent changes as in Fig. 2A, upper. Liver tissues of the saline-alone group were stained separately (scale bar: 200 μm) (n = 3–9 each). Lower: immunostaining (scale bar: 200 μm). Sircol assay and qRT-PCR were performed on the liver samples (n = 3–9 each). (C) Immunoblots and scanning densitometry. (D) H&E staining. Black arrows indicate ballooning degeneration of hepatocytes, whereas white arrows show infiltration of inflammatory cells and piecemeal necrosis of hepatocytes (scale bar: 200 μm) (n = 3–9 each). (E) HAI-Knodell scores and serum enzyme activities (n = 3–9 each). (F) Upper: Masson's trichrome staining. Mice were injected with LV-SMA-$G\alpha_{12}$-EGFP or MOCK through the tail vein. After 1 week, they were subjected to CCl_4 treatment for two weeks. Symbols represent changes as in Fig. 2A, upper (scale bar: 100 μm) (n = 5 each). Lower: H&E staining. Red arrows indicate eosinophilic degeneration, whereas white arrows show infiltration of inflammatory cells, and yellow arrows present vacuolar degeneration (scale bar: 100 μm) (n = 5 each). (G) Relative staining area fractions, HAI-Knodell scores, and serum enzyme activities (n = 5 each). (H) Immunoblots on primary hepatocytes and HSCs. At one week after injection of construct, hepatocytes and HSCs were freshly isolated from WT (left) or CCl_4-treated mice as in Fig. 1B right upper (right). (B, C and E) values represent the mean ± SEM. The statistical significance of the differences was determined by a two-tailed *t* -test (**p* <0.05, ***p* <0.01, significant *vs.* saline-treated WT mice; #*p* <0.05 and ##*p* <0.01, significant *vs.* CCl_4-treated WT mice injected with LV-con; and $*p* <0.05, $$*p* <0.01, significant *vs.* CCl_4-treated $G\alpha_{12}$ KO mice injected with LV-con, N.S., not significant). (G) Values represent the mean ± SEM (***p* <0.01, significant *vs.* vehicle-treated mice injected with LV-MOCK; and ##*p* <0.01, significant *vs.* CCl_4-treated WT mice injected with LV-MOCK). α-SMA, alpha-smooth muscle actin; CCl_4, carbon tetrachloride; $G\alpha_{12}$, guanine nucleotide-binding α-subunit 12; HSC, hepatic stellate cell; KO, knockout; qRT-PCR, quantitative reverse transcription PCR; WT, wild-type. (This figure appears in colour on the web.)

ATG12-5 conjugate levels were downregulated in $G\alpha_{12}$ KO primary HSCs (Fig. 4A, right). Consistently, either *in vitro* infection of LX-2 cells with $G\alpha_{12}$QL or HSC-specific infection of mice with $G\alpha_{12}$WT enhanced ATG12-5 conjugation (Fig. 4C and Fig. S5A), whereas Beclin1, ATG4B, and ATG7 levels changed minimally (Fig. S5B). ATG5 and ATG12 mRNA levels did not change significantly (Fig. S5C). Immunoblot results showed slight increases in LC3B-II, ATG12-5 conjugates, and p62 in liver homogenates from $G\alpha_{12}$ KO mice exhibiting HSC-specific $G\alpha_{12}$ overexpression compared with $G\alpha_{12}$ KO mice injected with

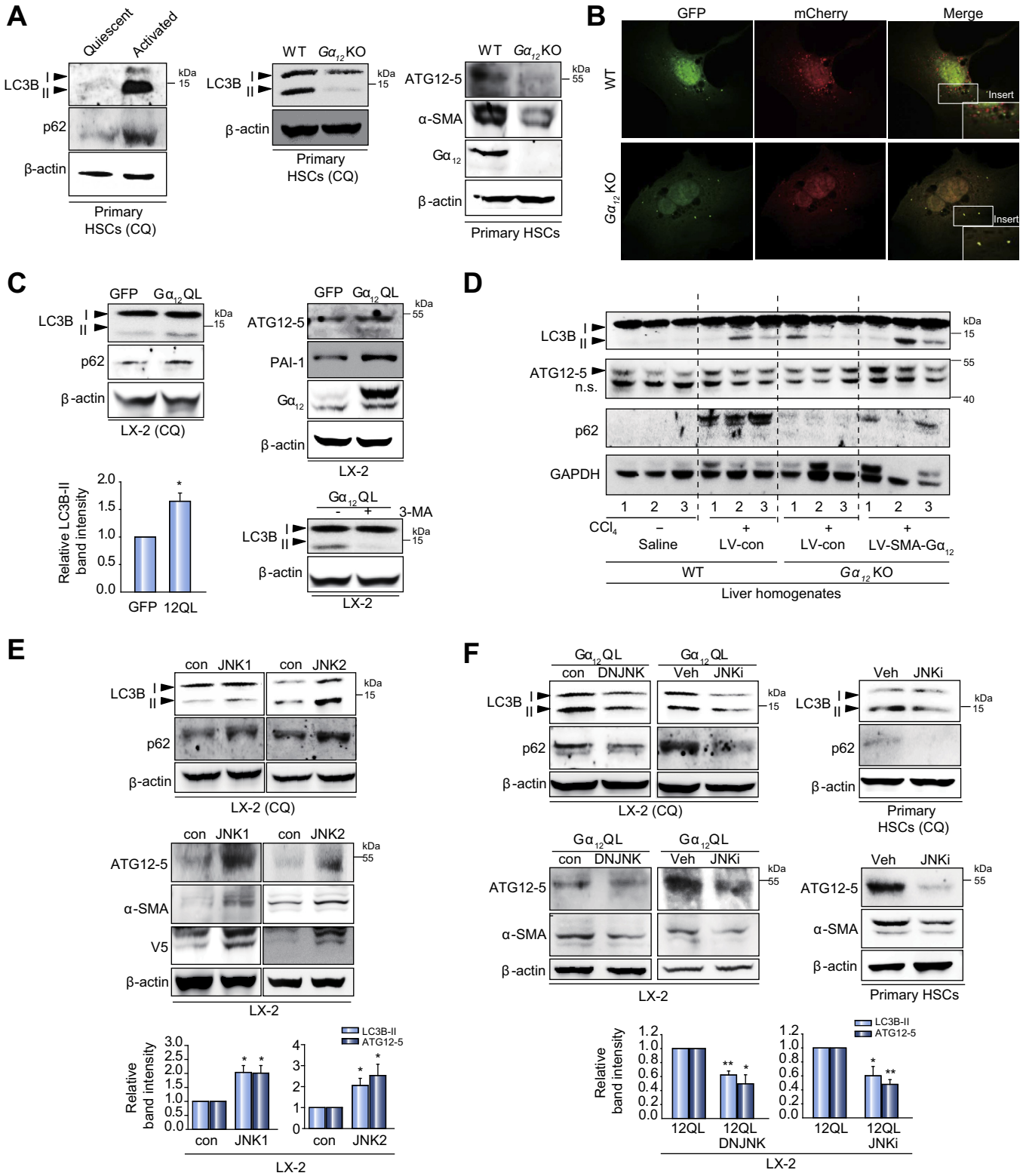

LV-con (Fig. 4D). In a separate experiment, LC3B-II was also elevated by a different construct specifically overexpressing $G\alpha_{12}$-GFP in HSCs, fortifying the link between $G\alpha_{12}$ and autophagy (Fig. S4B). LC3B colocalised with desmin in the liver sections (Fig. S5D).

Previously, we proposed JNK-dependent regulatory roles for $G\alpha_{12}$ in the induction of inflammatory signalling and cancer-cell biology.[5,6,19] Therefore, we sought to determine the role of JNK in ATG12-5 conjugation leading to autophagy activation downstream of $G\alpha_{12}$. Overexpression of either JNK1 or JNK2 increased LC3B-II, p62, ATG12-5, and α-SMA levels in LX-2 cells, whereas JNK inhibition using a dominant-negative mutant or chemical inhibitor (SP-600125) exerted the opposite effect against $G\alpha_{12}$-QL (Fig. 4E,F, left), which supported the ability of JNK1/2 to regulate the formation of ATG12-5 required for autophagy activation. JNK inhibitor treatment repressed LC3B, p62, ATG12-5, and α-SMA in primary HSCs, confirming the connections among $G\alpha_{12}$, JNK, and autophagy (Fig. 4F, right). Our results demonstrated that $G\alpha_{12}$ overexpression in HSCs facilitates the JNK-dependent formation of ATG12-5 to promote autophagy induction.

miR-16 dysregulation activates HSCs

To understand the molecular basis governing $G\alpha_{12}$ overexpression in HSCs, we measured $G\alpha_{12}$ transcript levels, and found that they were not increased in activated HSCs (Fig. 5A). Similar results were observed in animal liver samples and samples from patients (Fig. 6A,B). Therefore, it is likely that $G\alpha_{12}$ is post-transcriptionally regulated. miRs are major regulators of the post-transcriptional control of target cells.[20] To assess whether miRs mediate $G\alpha_{12}$-transcript levels, we used the TargetScan algorithm (Release 5.2, Whitehead Institute for Biomedical Research, MIT, MA, USA) to predict miR candidates targeting $G\alpha_{12}$ and then examined probabilities based on mirSVR scores (http://miRNA.org). Of these candidates, miR-16 had the highest affinity for $G\alpha_{12}$ (Fig. 5B) and was the most abundant miR observed in quiescent HSCs (Fig. 5C). Moreover, miR-16 levels were higher in quiescent HSCs than in hepatocytes (Fig. 5D). By contrast, the opposite was observed in the same samples for the expression of miR-122, which is abundant in hepatocytes. Intriguingly, miR-16 levels markedly diminished at Days 0–3 and then gradually decreased until Day 12 (Fig. 5E). In an additional assay, miR-16 levels were comparable between hepatocytes and Kupffer cells (Fig. S7A). The expression of other miRNAs predicted to inhibit $G\alpha_{12}$ and having the same or similar seed sequence(s) was also lower in these samples (Fig. S7B). These results implied that there is a link between miR-16 repression and HSC activation.

MiR-16 as a novel inhibitor of $G\alpha_{12}$

To assess whether miR-16 directly inhibits *de novo* $G\alpha_{12}$ synthesis (*i.e.* protein translation), we assessed the pairing between the miR-16 sequence and the $G\alpha_{12}$ 3′-untranslated region (UTR), and found almost complete complementarity. Moreover, the miR-16 recognition sites present in the 3′-UTR of $G\alpha_{12}$ mRNAs were highly conserved across different species (Fig. 6A). In LX-2 cells and primary HSCs, the ability of miR-16 to inhibit $G\alpha_{12}$ was supported by changes in $G\alpha_{12}$ levels following modulation of the miR-16 level by using an inhibitor or mimic (Fig. 6B). miR-16 inhibitor or mimic transfection appropriately modulated the expression of a Luciferase-$G\alpha_{12}$-3′-UTR construct in LX-2 or HEK293A cells (Fig. 6C and Fig. S7C). This effect was not seen when a mutant construct was used (Fig. 6D). These results indicated that miR-16 dysregulation results in $G\alpha_{12}$ overexpression in activated HSCs.

MiR-16 regulates autophagy and fibrosis

We then assessed the functional role of miR-16 in autophagy. Transfection with a miR-16 inhibitor enhanced autophagy flux in LX-2 cells, as shown by fluorescence assays (Fig. 7A). Consistently, miR-16 inhibitor transfection facilitated LC3B-II accumulation in LX-2 or primary HSCs (Fig. 7B). miR-16 modulation also changed α-SMA and/or PAI-1 levels. Additionally, miR-16 levels were significantly lower in liver samples from mice or patients with severe fibrosis compared with samples from control mice or patients with mild fibrosis (Ishak scores: 0–3 *vs.* 4–6) (Fig. 7C). Therefore, our data corroborated the regulatory effect of miR-16 on autophagy in HSCs and the resulting liver fibrosis.

$G\alpha_{12}$ and LC3 are upregulated in patients with cirrhosis

In an effort to reinforce our findings in a clinical situation, we examined $G\alpha_{12}$ and the markers of HSC activation and autophagy in cirrhotic and adjacent normal liver samples from patients with cancer. Staining for $G\alpha_{12}$, desmin, and LC3 occurred in similar regions of the liver sections, and their expression levels were higher in the cirrhotic regions (Fig. 8A), supporting the conclusion that $G\alpha_{12}$ upregulation in HSCs in conjunction with their activation facilitates the progression of liver fibrosis via the promotion of autophagy. Taken together, our data support the conclusion that miR-16 dysregulation

Fig. 4. $G\alpha_{12}$ activates autophagy in HSCs via ATG12-5 formation. (A) Left: immunoblots. Middle, Right: immunoblots on primary HSCs isolated from WT or *$G\alpha_{12}$* KO mice 48 h after a single CCl_4 treatment. HSCs were cultured in a growth medium for five days. (B) Fluorescent images for mCherry/GFP-LC3B puncta. Primary HSCs isolated from WT or *$G\alpha_{12}$* KO mice treated with CCl_4, as in (A), were cultured for three days, and then infected with ad-mCherry-GFP-LC3 for 24 h (magnification: 60×). (C) Left: immunoblots. LC3B-II levels were assessed by scanning densitometry (n = 3 each). Right upper: immunoblots. Right lower: immunoblots on LX-2 cells treated with 5 μM 3-MA (or vehicle) and CQ for 12 h following infection with ad-$G\alpha_{12}$QL (24 h). (D) Immunoblots on liver homogenates prepared as in Fig. 3A (n.s., non-specific band). (E) Immunoblots. LC3B-II and ATG12-5 levels were assessed by scanning densitometry (n = 3 each). (F) Left: immunoblots on LX-2 cells transfected with $G\alpha_{12}$QL in combination with DNJNK (or MOCK) for 48 h or those treated with vehicle or JNKi (10 μM) for 12 h following $G\alpha_{12}$QL infection for 24 h. Right: immunoblots on primary HSCs treated with vehicle or JNKi. Mouse HSCs were cultured in a growth medium for seven days. For immunoblottings for LC3B and p62, CQ (10 μM) was additionally treated for 12 h after transfection, or after infection plus 4 h serum starvation (for primary HSCs, CQ was additionally treated for 12 h at the indicated days, and cells were also exposed to CQ 4 h before JNKi treatment). (C, E, and F) Values represent the mean ± SEM. The statistical significance of the differences was determined by a two-tailed *t* test (*p <0.05, **p <0.01, significant compared with respective controls). α-SMA, alpha-smooth muscle actin; ATG, autophagy-related gene; CCl_4, carbon tetrachloride; CQ, chloroquine; $G\alpha_{12}$, guanine nucleotide-binding α-subunit 12; GAPDH, glyceraldehyde 3-phosphate dehydrogenase; GFP, green fluorescent protein; HSC, hepatic stellate cell; JNKi, c-Jun N-terminal kinase inhibitor; WT, wild-type. (This figure appears in colour on the web.)

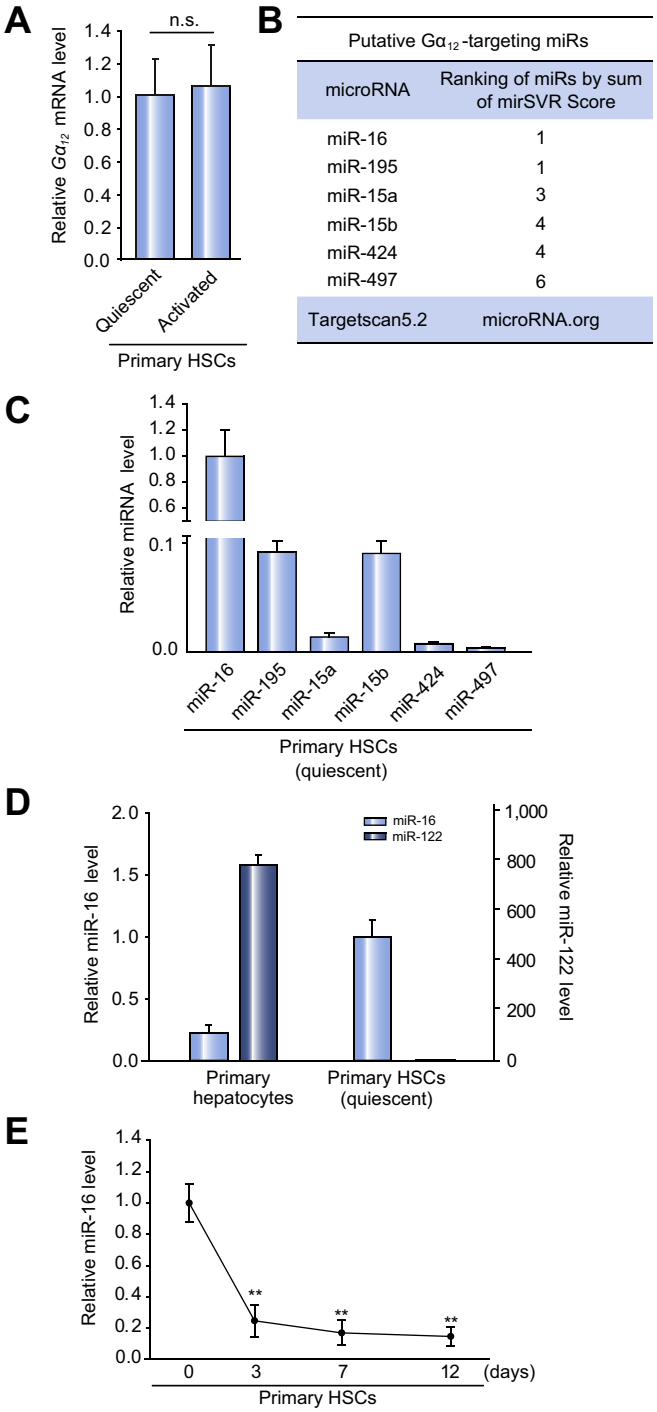

Fig. 5. miR-16 is dysregulated during HSC activation. (A) qRT-PCR assay (n = 3 each). (B) miRs putatively targeting $G\alpha_{12}$. The candidate miRs were ranked by the sum of mirSVR scores obtained using a miR algorithm. (C–E) qRT-PCR assays (n = 3–4 each). (A, E) Values represent the mean ± SEM. The statistical significance of the differences was determined by a two-tailed *t* test (**p <0.01, significant compared with quiescent or freshly isolated primary HSCs, N.S., not significant). $G\alpha_{12}$, guanine nucleotide-binding α-subunit 12; HSC, hepatic stellate cell; miR, microRNA; qRT-PCR, quantitative reverse transcription PCR.

causes $G\alpha_{12}$ overexpression, which activates HSCs by facilitating autophagy, demonstrating the link between G-protein signalling and the progression of liver fibrosis (Fig. 8B).

Discussion

HSC activation is mediated by extracellular ligands.[21,22] In addition, GPCR-signalling pathways have a profound effect on cell behaviour during fibrogenesis. Levels of GPCR ligands are elevated in fibrotic livers compared with healthy controls, and most GPCRs activated by ligands are coupled with $G\alpha_{12}$.[7,8] Despite the known effects of $G\alpha_{12}$ on cell proliferation and migration,[5] the basis for $G\alpha_{12}$ signalling in liver fibrosis has remained unknown. Our results demonstrated that $G\alpha_{12}$ was overexpressed in HSCs under conditions of liver fibrosis. Proteomic data showing that $G\alpha_{12}$ was most-strongly expressed in HSCs among different Gα members support the regulatory role of $G\alpha_{12}$ in HSC *trans*-differentiation, as also suggested by immunostaining data from two different animal models of fibrosis. Our findings implied that signals converging from different GPCRs activated by fibrogenic mediators in HSCs were amplified by increased $G\alpha_{12}$ levels. This idea was supported by observations that $G\alpha_{12}$ deficiency attenuated fibrotic severity and accompanying inflammatory responses against toxicant challenges and that these events were reversible by HSC-specific gene delivery. Furthermore, we observed that $G\alpha_{13}$, another $G\alpha_{12}$ family member, was not comparably induced in fibrosis samples and activated HSCs (Fig. S8), suggesting a greater role for $G\alpha_{12}$ in HSC activation. cDNA microarrays using liver tissues from WT and $G\alpha_{12}$-null mice revealed that $G\alpha_{12}$ has a role in mitochondrial energy expenditure (TH Kim *et al.*, unpublished data). In another study, HSC activation was accompanied by mitochondrial biogenesis (AY Kim *et al.*, unpublished data), supporting the concept that $G\alpha_{12}$ contributes to HSC activation in conjunction with fuel oxidation. However, *$G\alpha_{12}$* KO mice were viable and fertile without any apparent phenotypic changes.[23]

Our finding that HSC-specific delivery of $G\alpha_{12}$ facilitated liver fibrosis in *$G\alpha_{12}$* KO animals strengthened the predicted functional role of $G\alpha_{12}$ overexpression in HSCs in the progression of fibrosis. This outcome agreed with the finding that $G\alpha_{12}$ members regulate the transforming growth factor beta 1 (*Tgf-β1*) gene via Activator protein 1.[24] Here, HSC-specific $G\alpha_{12}$ overexpression partially reversed the protective effects of *$G\alpha_{12}$* KO on ALT, AST, and LDH activities. In addition, the lack of statistical significance associated with our first experiment might have resulted from variations in the animals used and/or the involvement of other types of cell deficient in $G\alpha_{12}$ (*e.g.* macrophages). However, the additional results based on our HSC-specific $G\alpha_{12}$WT-EGFP construct provided additional evidence for the effect of $G\alpha_{12}$ on HSCs and liver injury.

Damaged hepatocytes contribute to the pathogenesis of liver fibrosis. In turn, activated HSCs produce TGF-β and other cytokines, facilitating hepatocyte injury, macrophage infiltration and activation, and HSC activation, which accelerate disease progression.[25] Indeed, $G\alpha_{12}$ overexpression in HSCs nullified the beneficial effect of *$G\alpha_{12}$* KO on hepatic inflammation and injury. Given that $G\alpha_{12}$ aggravates inflammatory signalling through cyclo-oxygenase-2 and inducible nitric oxide synthases,[6,19] $G\alpha_{12}$ in macrophages might also contribute to inflammation and thereby HSC activation; however, this requires further investigation using other types of cell to provide a more comprehensive understanding of this disease. Nonetheless, the concept is supported by liver fibrosis being a steadily progressive disease involving the complicated interplay between hepatocytes and other cell populations.[26]

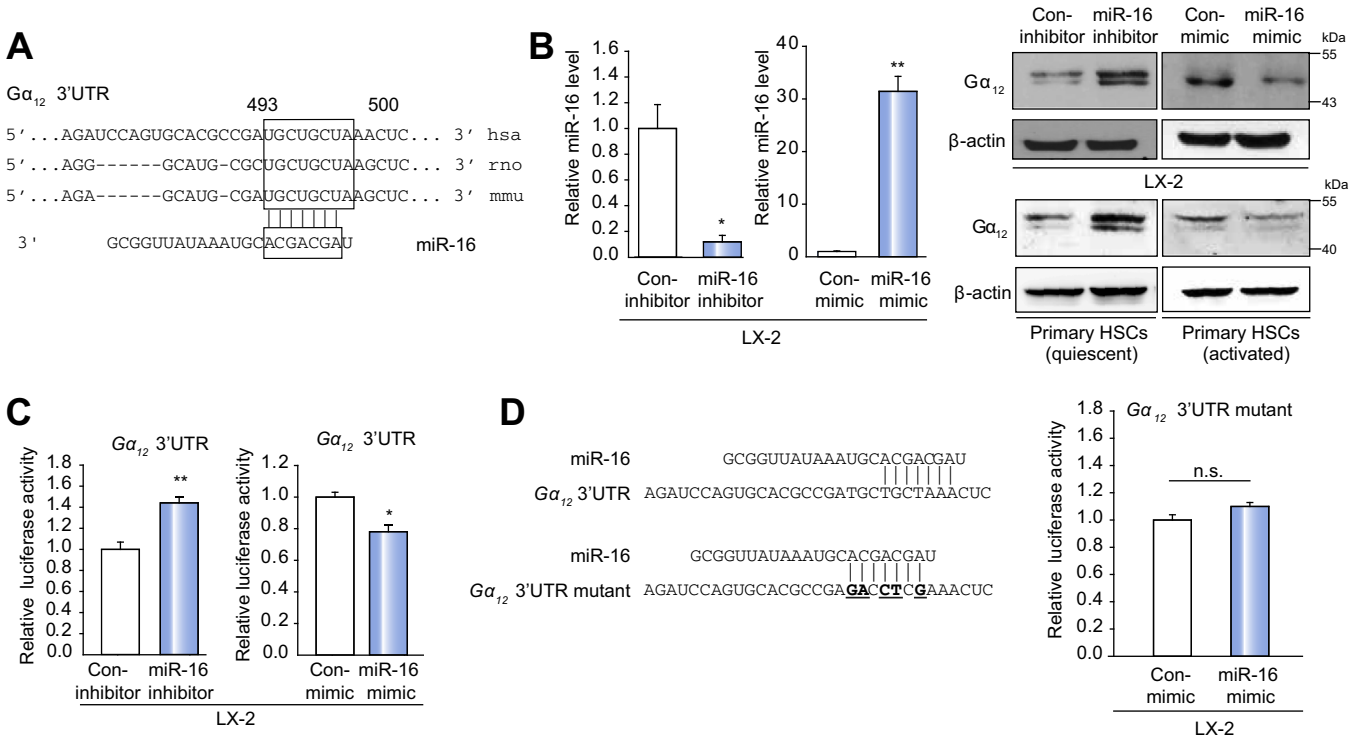

Fig. 6. miR-16 directly inhibits Gα$_{12}$. (A) Alignments of miR-16 binding to the 3′-UTRs of Gα$_{12}$ mRNAs. (B) Left: qRT-PCR for miR-16 (n = 3 each). Right: immunoblots for Gα$_{12}$. (C) 3′-UTR reporter assays (n = 3 each). (D) hsa-miR-16 sequence and its target sequences in the Gα$_{12}$ 3′-UTR, or Gα$_{12}$ 3′-UTR mutant (changed bases are underlined), and reporter assays (n = 3 each). (B–D) Values represent the mean ± SEM. The statistical significance of the differences was determined by a two-tailed *t* test (**p* <0.05 and ***p* <0.01, significant as compared with respective controls, N.S., not significant). Gα$_{12}$, guanine nucleotide-binding α-subunit 12; HSC, hepatic stellate cell; qRT-PCR, quantitative reverse transcription PCR; miR, microRNA; UTR, untranslated region; WT, wild-type.

Autophagy provides the energy required to support HSC *trans*-differentiation through the mobilisation and breakdown of lipid droplets and mitochondrial β-oxidation.[10] Such events would allow HSCs to meet the cellular energy demands conferred by cell proliferation, repair, and the maintenance of energy homeostasis.[10] Therefore, autophagy might be a modulator of signalling pathways related to the differentiation of several cell types, including HSCs.[10,27] Nevertheless, the underlying basis by which autophagy controls HSC activation has remained elusive. Here, we reported the ability of Gα$_{12}$ overexpressed in HSCs to control autophagy; this event depended on increases in a ATG12-5 conjugate, consistent with reports that some ligands that activate GPCRs coupled with Gα$_{12}$ also stimulate autophagy.[12,13] The hypothesis that Gα$_{12}$ promotes autophagy in HSCs was reinforced by changes in LC3B-II and ATG12-5 levels in liver homogenates following HSC-specific Gα$_{12}$ delivery. Thus, Gα$_{12}$ is likely to have a role in autophagic signal amplification through increases in the ATG12-5 conjugate, as supported by the observation that the ATG12-5 conjugate, but not unconjugated ATG12 or ATG5, enhances LC3-II formation.[28]

JNK activation upregulates α-SMA in response to TGF-β, platelet-derived growth factor, and AngII.[29] JNK also participates in autophagy, including interactions with ATGs and the induction and/or activation of Beclin1, ATG7, and ATG5.[30] Previously, JNK was identified as a kinase regulated by the Gα$_{12}$-signalling pathway involved in various biological events.[5,6,19] In our study, the JNK pathway downstream of Gα$_{12}$ regulated autophagy by promoting ATG12-5 conjugation. Despite the reports of conflicting roles of JNK isoforms in HSC proliferation and activation,[29] our findings showed that JNK1 and JNK2 were both involved in ATG12-5 formation. Additionally, their activities were equally increased in the cells transfected with Gα$_{12}$-QL.[31] The detailed molecular basis associated with JNK regulation of ATG12-5 remains unknown. Given that JNK1/2 are involved in various mechanisms related to the pathogenesis of liver injury with shared and different functions,[32,33] additional research is needed to determine the discrete roles of JNK isoforms during the initiation and progression of HSC *trans*-differentiation.

Another important finding of our study involved the identification of miR-16 as an upstream Gα$_{12}$ regulator. Our findings that miR-16 was markedly repressed during HSC activation and inhibited Gα$_{12}$ by binding to Gα$_{12}$ mRNA with high affinity supported the conclusion that miR-16 dysregulation contributes to HSC activation through Gα$_{12}$ overexpression. This was supported by changes in autophagic biomarker and flux. The time-course data for Gα$_{12}$ and miR-16 in HSCs corresponded to each other, being consistent with the idea that Gα$_{12}$ overexpression results from miR-16 dysregulation. Moreover, we validated the relationship between miR-16 dysregulation and liver fibrosis using samples from humans. As a liver-enriched miR, miR-16 regulates HSC proliferation,[34] further supporting the importance of miR-16 in HSC biology.

Of note, miR-16 levels were higher in quiescent HSCs than in hepatocytes. Given that the number of HSCs increases with activation, whereas the number of hepatocytes declines,[1] modulation of miR-16 in HSCs would contribute more to liver fibrosis than in hepatocytes. We also found that miR-16 levels were comparable between hepatocytes and Kupffer cells. Given that

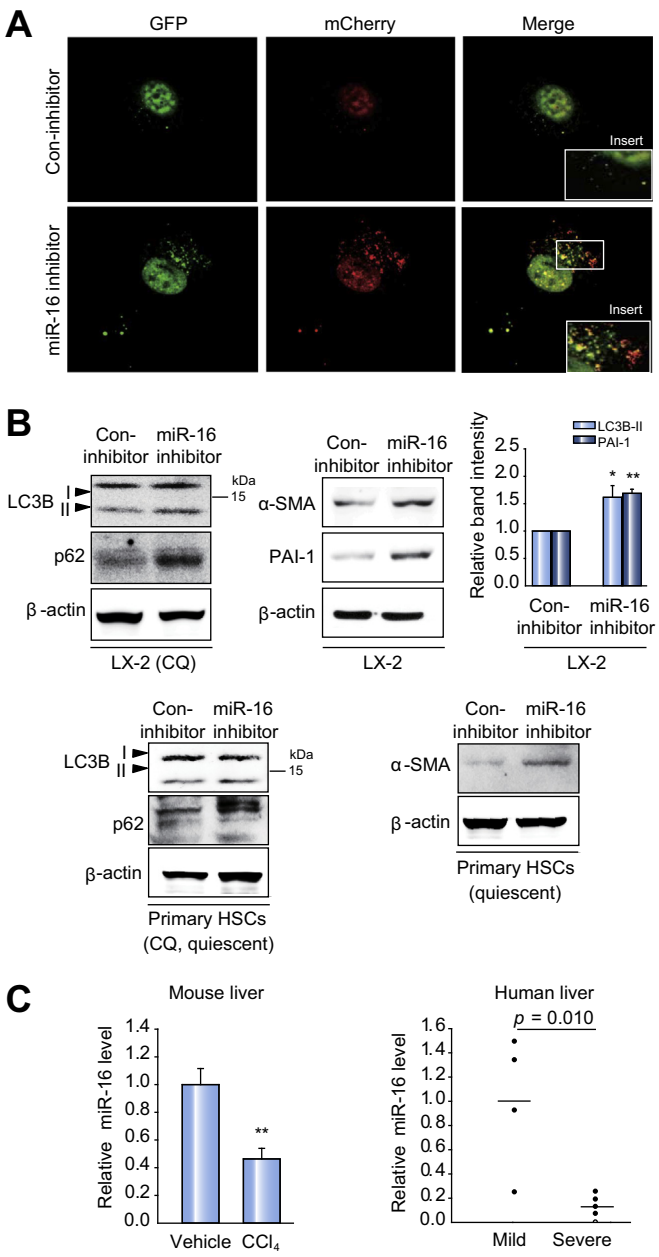

Fig. 7. Dysregulation of miR-16 promotes autophagy in HSCs. (A) Fluorescent images for mCherry/GFP-LC3B puncta (magnification: 60×). (B) Upper: immunoblots and scanning densitometry (n = 3 each). Lower: immunoblots on transfected quiescent HSCs. For immunoblottings for LC3B and p62, the cells were additionally treated with 10 μM CQ for 12 h after transfection. (C) qRT-PCR assays in liver samples prepared as in Fig. 1B (left) (n = 3–4 each) or in the liver sections of patients with either mild or severe fibrosis (Ishak scores: 0–3 *vs.* 4–6; right) (n = 4–5 each). (B upper right and C left), values represent the mean ± SEM. The statistical significance of the differences was determined by a two-tailed *t* test (**p* <0.05, ***p* <0.01, significant compared with respective controls). (C right) Means are indicated. α-SMA, alpha-smooth muscle actin; CQ, chloroquine; $G\alpha_{12}$, guanine nucleotide-binding α-subunit 12; GFP, green fluorescent protein; HSC, hepatic stellate cell; miR, microRNA; qRT-PCR, quantitative reverse transcription PCR; WT, wild-type. (This figure appears in colour on the web.)

the levels of $G\alpha_{12}$ were lower in Kupffer cells than in hepatocytes, we speculate that miR-16 in Kupffer cells would have a smaller effect on fibrosis than miR-16 in hepatocytes. Nonetheless, our data do not exclude the possible role of miR-16 in $G\alpha_{12}$ in other types of liver cells.

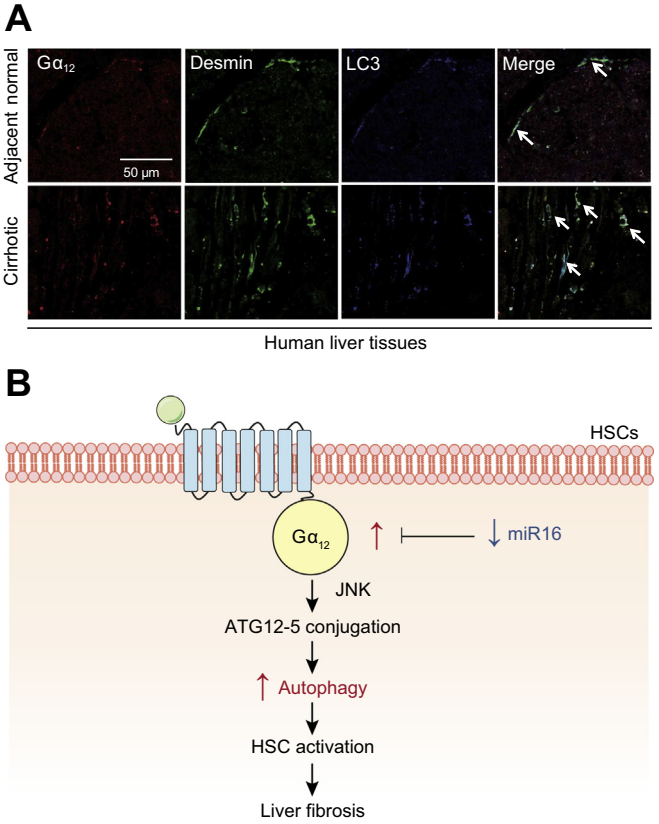

Fig. 8. Immunostaining for $G\alpha_{12}$, desmin and LC3 in cirrhotic specimens and adjacent normal specimens from patients with cancer. (A) Immunostaining (scale bar: 50 μm). White arrows indicate colocalisation of $G\alpha_{12}$, desmin, and LC3. The result was confirmed using another set of human samples. (B) A schematic diagram illustrating the proposed mechanism by which $G\alpha_{12}$ overexpression promotes HSC activation. $G\alpha_{12}$, guanine nucleotide-binding α-subunit 12. (This figure appears in colour on the web.)

Targeting multiple sites of miRNA enhances the degree of target gene inhibition.[35] We observed downregulation of miR-15a, miR-15b, miR-195, miR-424, and miR-497 in activated HSCs. Given that these miRs have different genomic locations and have the same seed sequence as miR-16, they might also affect *de novo* $G\alpha_{12}$ synthesis.[35] Two sites of the same or different miRNAs located closely to each other act synergistically.[36] However, the above-mentioned miRs have the same seed sequence, therefore binding the same location in the 3′-UTR of $G\alpha_{12}$ mRNA. HSC *trans*-differentiation and the consequent changes in expression of genes encoding ECM proteins are governed by various miRNAs, including miR-29b, miR-150, and miR-194.[37,38] Therefore, it is likely that HSC activation is regulated by the pleiotropic action of multiple miRs.

We found that the level of α-SMA in LX-2 was comparable to that in quiescent HSCs, but was lower than in activated HSCs (data not shown). LX-2 cells appear to contain fewer lipids than activated HSCs, but more than quiescent HSCs.[39] $G\alpha_{12}$QL repeatedly increased autophagy in LX-2, supporting the notion that the cells are not fully activated. In our study, the results obtained using LX-2 were almost identical to those in primary HSCs, demonstrating that $G\alpha_{12}$ overexpression by miR-16 dysregulation enhances autophagy in HSCs. This idea was reinforced by the association of $G\alpha_{12}$, desmin, and LC3 in human samples. In another study, $G\alpha_{12}$ crosstalked with integrin-linked kinase.[40] Given that $G\alpha_{12}$ promotes reactive oxygen

species production[41] and inflammation,[6,19] HSC activation by $G\alpha_{12}$ might rely on these factors. However, in our experiment, treatment with TGF-β, PDGF, tert-butylhydroperoxide, or tumour necrosis factor-α failed to change $G\alpha_{12}$ or miR-16 levels (data not shown). Given that liver fibrosis induces drastic changes in the tissue microenvironment,[26] we hypothesise that multiple fibrogenic stimuli have direct and/or indirect effects on the $G\alpha_{12}$-dependent activation of HSCs. Collectively, miR-16 dysregulation elicits $G\alpha_{12}$ overexpression, which activates HSCs by facilitating autophagy via ATG12-5 conjugation. Thus, $G\alpha_{12}$ and its regulatory molecules could serve as new targets for the prevention and treatment of liver fibrosis.

Financial support

This work was supported by National Research Foundation (NRF) grants funded by the Government of South Korea (MSIP) (NRF-2015R1A2A1A10052663) and the NRF-JSPS program.

Conflict of interest

The authors declare that they have no conflict of interest to report. Please refer to the accompanying ICMJE disclosure forms for further details.

Authors' contributions

KMK, CYH, JYK, SSC, YSK, JHK, and JML acquired experimental data. SCL, KWK, JSK, and SJH provided administrative, technical, or material support. KMK, CYH, SHK, and SGK were involved in the study concept and design. KMK and SGK drafted the manuscript. SGK contributed to writing the manuscript, study supervision, and obtaining funding.

Supplementary data

Supplementary data associated with this article can be found, in the online version, at https://doi.org/10.1016/j.jhep.2017.10.011.

References

Author names in bold designate shared co-first authorship.

[1] **Yin C**, **Evason KJ**, Asahina K, Stainier DY. Hepatic stellate cells in liver development, regeneration, and cancer. J Clin Invest 2013;123:1902–1910.
[2] Friedman SL. Hepatic stellate cells: protean, multifunctional, and enigmatic cells of the liver. Physiol Rev 2008;88:125–172.
[3] Tacke F, Weiskirchen R. Update on hepatic stellate cells: pathogenic role in liver fibrosis and novel isolation techniques. Expert Rev Gastroenterol Hepatol 2012;6:67–80.
[4] Trzaskowski B, Latek D, Yuan S, Ghoshdastider U, Debinski A, Filipek S. Action of molecular switches in GPCRs–theoretical and experimental studies. Curr Med Chem 2012;19:1090–1109.
[5] **Jung HS**, **Seo YR**, Yang YM, Koo JH, An J, Lee SJ, et al. $G\alpha_{12}$gep oncogene inhibits FOXO1 in hepatocellular carcinoma as a consequence of miR-135b and miR-194 dysregulation. Cell Signal 2014;26:1456–1465.
[6] Kang KW, Choi SY, Cho MK, Lee CH, Kim SG. Thrombin induces nitric-oxide synthase via $G\alpha_{12/13}$-coupled protein kinase C-dependent I-κBα phosphorylation and JNK-mediated I-κBα degradation. J Biol Chem 2003;278:17368–17378.
[7] Duplantier JG, Dubuisson L, Senant N, Freyburger G, Laurendeau I, Herbert JM, et al. A role for thrombin in liver fibrosis. Gut 2004;53:1682–1687.
[8] Bataller R, Sancho-Bru P, Gines P, Lora JM, Al-Garawi A, Sole M, et al. Activated human hepatic stellate cells express the renin-angiotensin system and synthesize angiotensin II. Gastroenterology 2003;125:117–125.
[9] Kelly P, Casey PJ, Meigs TE. Biologic functions of the G12 subfamily of heterotrimeric g proteins: growth, migration, and metastasis. Biochemistry 2007;46:6677–6687.
[10] Hernandez-Gea V, Ghiassi-Nejad Z, Rozenfeld R, Gordon R, Fiel MI, Yue Z, et al. Autophagy releases lipid that promotes fibrogenesis by activated hepatic stellate cells in mice and in human tissues. Gastroenterology 2012;142:938–946.
[11] Kabeya Y, Mizushima N, Ueno T, Yamamoto A, Kirisako T, Noda T, et al. LC3, a mammalian homologue of yeast Apg8p, is localized in autophagosome membranes after processing. EMBO J 2000;19:5720–5728.
[12] Yadav A, Vallabu S, Arora S, Tandon P, Slahan D, Teichberg S, et al. ANG II promotes autophagy in podocytes. Am J Physiol Cell Physiol 2010;299:C488–C496.
[13] Chang CL, Ho MC, Lee PH, Hsu CY, Huang WP, Lee H. S1P(5) is required for sphingosine 1-phosphate-induced autophagy in human prostate cancer PC-3 cells. Am J Physiol Cell Physiol 2009;297:C451–C458.
[14] Azimifar SB, Nagaraj N, Cox J, Mann M. Cell-type-resolved quantitative proteomics of murine liver. Cell Metab 2014;20:1076–1087.
[15] Koo JH, Lee HJ, Kim W, Kim SG. Endoplasmic reticulum stress in hepatic stellate cells promotes liver fibrosis via PERK-mediated degradation of HNRNPA1 and up-regulation of SMAD2. Gastroenterology 2016;150:181–193.
[16] **Thoen LF**, **Guimaraes EL**, Dolle L, Mannaerts I, Najimi M, Sokal E, et al. A role for autophagy during hepatic stellate cell activation. J Hepatol 2011;55:1353–1360.
[17] Klionsky DJ, Abdelmohsen K, Abe A, Abedin MJ, Abeliovich H, Acevedo Arozena A, et al. Guidelines for the use and interpretation of assays for monitoring autophagy (3rd edition). Autophagy 2016;12:1–222.
[18] Levine B, Klionsky DJ. Development by self-digestion: molecular mechanisms and biological functions of autophagy. Dev Cell 2004;6:463–477.
[19] Ki SH, Choi MJ, Lee CH, Kim SG. $G\alpha_{12}$ specifically regulates COX-2 induction by sphingosine 1-phosphate. Role for JNK-dependent ubiquitination and degradation of IκBα. J Biol Chem 2007;282:1938–1947.
[20] Wang XW, Heegaard NH, Orum H. MicroRNAs in liver disease. Gastroenterology 2012;142:1431–1443.
[21] Breitkopf K, Godoy P, Ciuclan L, Singer MV, Dooley S. TGF-β/Smad signaling in the injured liver. Z Gastroenterol 2006;44:57–66.
[22] **Breitkopf K**, **Roeyen C**, Sawitza I, Wickert L, Floege J, Gressner AM. Expression patterns of PDGF-A, -B, -C and -D and the PDGF-receptors α and β in activated rat hepatic stellate cells (HSC). Cytokine 2005;31:349–357.
[23] **Gu JL**, **Muller S**, Mancino V, Offermanns S, Simon MI. Interaction of $G\alpha_{12}$ with $G\alpha_{13}$ and Gαq signaling pathways. Proc Natl Acad Sci U S A 2002;99:9352–9357.
[24] **Lee SJ**, **Yang JW**, Cho IJ, Kim WD, Cho MK, Lee CH, et al. The gep oncogenes, $G\alpha_{12}$ and $G\alpha_{13}$, upregulate the transforming growth factor-β1 gene. Oncogene 2009;28:1230–1240.
[25] Hernandez-Gea V, Friedman SL. Pathogenesis of liver fibrosis. Annu Rev Pathol 2011;6:425–456.
[26] Vinas O, Bataller R, Sancho-Bru P, Gines P, Berenguer C, Enrich C, et al. Human hepatic stellate cells show features of antigen-presenting cells and stimulate lymphocyte proliferation. Hepatology 2003;38:919–929.
[27] Mizushima N, Levine B. Autophagy in mammalian development and differentiation. Nat Cell Biol 2010;12:823–830.
[28] Hanada T, Noda NN, Satomi Y, Ichimura Y, Fujioka Y, Takao T, et al. The Atg12-Atg5 conjugate has a novel E3-like activity for protein lipidation in autophagy. J Biol Chem 2007;282:37298–37302.
[29] Kluwe J, Pradere JP, Gwak GY, Mencin A, De Minicis S, Osterreicher CH, et al. Modulation of hepatic fibrosis by c-Jun-N-terminal kinase inhibition. Gastroenterology 2010;138:347–359.
[30] Zhou YY, Li Y, Jiang WQ, Zhou LF. MAPK/JNK signalling: a potential autophagy regulation pathway. Biosci Rep 2015;35.
[31] Juneja J, Cushman I, Casey PJ. G12 signaling through c-Jun NH2-terminal kinase promotes breast cancer cell invasion. PLoS One 2011;6:e26085.
[32] **Hirosumi J**, **Tuncman G**, Chang L, Gorgun CZ, Uysal KT, Maeda K, et al. A central role for JNK in obesity and insulin resistance. Nature 2002;420:333–336.
[33] Chen N, She QB, Bode AM, Dong Z. Differential gene expression profiles of Jnk1- and Jnk2-deficient murine fibroblast cells. Cancer Res 2002;62:1300–1304.

[34] Guo CJ, Pan Q, Li DG, Sun H, Liu BW. MiR-15b and miR-16 are implicated in activation of the rat hepatic stellate cell: an essential role for apoptosis. J Hepatol 2009;50:766–768.
[35] Lai EC. Predicting and validating microRNA targets. Genome Biol 2004;5:115.
[36] **Grimson A**, **Farh KK**, Johnston WK, Garrett-Engele P, Lim LP, Bartel DP. MicroRNA targeting specificity in mammals: determinants beyond seed pairing. Mol Cell 2007;27:91–105.
[37] Venugopal SK, Jiang J, Kim TH, Li Y, Wang SS, Torok NJ, et al. Liver fibrosis causes downregulation of miRNA-150 and miRNA-194 in hepatic stellate cells, and their overexpression causes decreased stellate cell activation. Am J Physiol Gastrointest Liver Physiol 2010;298:G101–G116.
[38] Ogawa T, Iizuka M, Sekiya Y, Yoshizato K, Ikeda K, Kawada N. Suppression of type I collagen production by microRNA-29b in cultured human stellate cells. Biochem Biophys Res Commun 2010;391:316–321.
[39] Lee TF, Mak KM, Rackovsky O, Lin YL, Kwong AJ, Loke JC, et al. Downregulation of hepatic stellate cell activation by retinol and palmitate mediated by adipose differentiation-related protein (ADRP). J Cell Physiol 2010;223:648–657.
[40] Shafiei MS, Rockey DC. The function of integrin-linked kinase in normal and activated stellate cells: implications for fibrogenesis in wound healing. Lab Invest 2012;92:305–316.
[41] Fujii T, Onohara N, Maruyama Y, Tanabe S, Kobayashi H, Fukutomi M, et al. $G\alpha_{12/13}$-mediated production of reactive oxygen species is critical for angiotensin receptor-induced NFAT activation in cardiac fibroblasts. J Biol Chem 2005;280:23041–23047.